Pulsed NMR Study of Elastomeric Block Copolymer under Deformation

KENZO FUKUMORI, TOSHIO KURAUCHI, and OSAMI KAMIGAITO, *Toyota Central Research and Development Laboratories, Inc., Nagakute-cho, Aichi-gun, Aichi-ken, 480-11, Japan*

Synopsis

Deformation behavior of an elastomeric styrene–butadiene–styrene block copolymer (SBS) is studied by pulsed NMR techniques, and is related to lifetime distributions and the change of the microstructure in the stress relaxation process. By the measurement of spin–spin relaxation time, it is found that polybutadiene (PB) chains in the vicinity of polystyrene (PS) domains come to be in more constrained conformations with stretching than those remote from the domains mainly through the intramolecular interactions, followed by the enlargement of the constrained regions, which reflects the roles of both crosslinks and filler particles in crosslinked rubbers. In the stress relaxation process, however, the mean lifetime for SBS at the critical strain is longer than that at lower strain in contrast with the results for the crosslinked rubbers. It is estimated that the differences between the failure behaviors of SBS and those of the conventional crosslinked rubbers may be mainly caused by the characteristic change of the microstructure (the disruption of the weak interconnections between the spherical PS domains with high energy dissipation) in SBS on deformation, associated with the limited extensibility of the PB chains between the adjacent PS domains. It becomes clear that the pulsed NMR method complements the mechanical measurements with a more precise information on the heterogeneity in the rubbery polymers under deformation.

INTRODUCTION

Many useful heterogeneous polymers (e.g., polymer blends, block copolymers, filled polymers) are widely used in practical applications, and the microstructures in the polymers exert a great influence on the physical properties of the materials. Because of the immiscible nature of the multicomponent polymers, the heterogeneous structures in the materials are sensitively controlled by both the composition of the systems and processing conditions. It is of great interest to elucidate the relations between the structure of the heterogeneous polymers and their properties.

In the heterogeneous polymers, a crosslinked rubber uniquely displays large recoverable deformation (i.e., rubber elasticity) dependent on the changes of conformation of long-chain molecules in striking contrast to the elasticity of ordinary solid polymers such as semicrystalline and glassy polymers.[1] The crosslinked rubber is commonly filled with particulate fillers such as carbon black to increase the strength of the rubbery matrix more than tenfold. There have been many studies on the thermodynamic implications of the phenomenon of rubber elasticity, but some features of the elastic response of rubbery materials are still not fully understood, especially for the filled

Journal of Applied Polymer Science, Vol. 38, 1313–1334 (1989)
 CCC 0021-8995/89/071313-22$04.00

system, i.e., the roles of the crosslinks and filler particles in the network chains under deformation.

An elastomeric A–B–A type of block copolymer[2,3] in which hard domains serve as both crosslinks and reinforcing fillers is considered to be a most suitable model for the basic understanding of the deformation behavior of the crosslinked rubber because of its regularity in the microstructure, and the precise information on the domain size and domain shape can be obtained from other methods such as transmission electron microscopy (TEM), small angle X-ray scattering (SAXS), and so on.

There have been many studies of the time-dependent structure–property relationships of elastomeric block copolymers (i.e., thermoplastic elastomers), especially on those of the A–B–A type of block copolymers.[4–17] As for the failure behaviors of the thermoplastic elastomers, previous studies have been focused mainly on the ultimate tensile properties of these materials.[10–17] There were few reports on the long-term failure behaviors of the materials important for the practical use, such as those in creep and stress relaxation processes. The long-term failure properties of the solids are sensitively controlled by the microscopic change of the structure than the overall mechanical properties, and provide a useful hint on the elucidation of the change of the microstructure in the materials. In the previous paper,[18] the failure behaviors of an elastomeric styrene–butadiene–styrene triblock copolymer (SBS) added with plasticizer in the creep and stress relaxation processes were studied by the statistical analysis of lifetime distributions, on the basis of the stochastic theory proposed for crosslinked rubbers.[19] It is clarified that in SBS the polystyrene (PS) component, dispersed in a matrix of polybutadiene (PB), serves as both a physical crosslink and a reinforcing filler, and that the wear-out failure occurs in SBS in similar manner to that in a crosslinked rubber filled with carbon black particles. In the stress relaxation process, however, it was found that the mean lifetime at the critical strain is longer than that at lower strain in contrast with the results for the crosslinked rubbers.[19] Hence, the detailed understanding of this novel failure behavior of SBS seems to be of great importance to clarify the roles of the crosslinks and filler particles in both chemically crosslinked rubbers and physically crosslinked ones.

Rubbery polymers behave like a liquid and exhibit the molecular mobility of the liquid state. In the elastomeric block copolymers which show rubber elasticity, the rubbery long-chain molecules between the hard domains have the freedom to take up the variety of statistical conformations, and the secondary forces between the molecules (i.e., intermolecular interaction) must be weak to achieve the inherent elasticity, apart from the fact that all the molecules are linked together physically through the hard domains. The rubbery chains will take up random conformations in a stress-free state, but assume somewhat oriented conformations if tensile forces are applied at their ends.

For the study of the molecular orientation in the rubbery polymers, a variety of spectroscopic techniques has recently become available, encompassing infrared dichroism, deuterium (^{2}H) nuclear magnetic resonance (NMR) spectroscopy, wide-angle X-ray scattering, etc.[20,21] On the other hand, a pulsed NMR method provides a sensitive probe of the molecular state of a

nuclear environment through the short range nature of the magnetic dipolar interactions, closely connected with the constrained conformations and molecular orientation of the rubbery chains under deformation. Moreover, by the pulsed NMR measurement, the information on the interface structure of the heterogeneous polymers and the inhomogeneous distribution of the plasticizer in the rubbery matrix important for the physical properties of the block copolymers can be obtained directly related to motional states of molecules. Pulsed NMR method seems to be one of the most useful tools for studying heterogeneous polymer systems.[22-25] The molecular mobility of each component and the fraction of the component can be directly estimated by the measurement of the spin–spin relaxation time T_2.

Hence, it is expected that the pulsed NMR techniques may give direct information on the molecular mobility of the block copolymers closely connected with the deformation behavior of rubbery chains in those. A number of NMR measurements have been reported on the heterogeneous structure of block copolymers.[26-30] However, there were few studies on the relationship between the mechanical properties of the block copolymers and microscopic molecular mobility of those.

In this study, the T_2 measurements for SBS in stretched states were carried out, and were related to the mechanical measurements and the change of the microstructure observed by TEM. Then, the heterogeneity in SBS and the deformation and failure mechanisms of SBS in the stress relaxation process were discussed in order to understand the deformation behaviors of the network chains between adjacent points of attachment (crosslink or filler particle) in the crosslinked rubbers.

EXPERIMENTAL

SBS used in this study was Cariflex TR4113 (Shell Chemical Co.; weight-average molecular weight of 8.0×10^4, PS/PB = 38/62 wt %), added with 31.5 wt % naphthenic oil (cycloparaffins and their derivatives) for processing aids and extenders for PB phase. Sheets ($150 \times 150 \times \sim 1$ mm) were prepared by compression molding at 120°C for 5 min. Ring specimens (18.6 inside, 20.0 outside) were punched out from the sheets.

Tensile and Stress Relaxation Experiments

Tensile and stress relaxation experiments were carried out at 23°C under ambient atmosphere. In the tensile experiment, a ring specimen was strained at a constant rate of 100 mm/min. In the stress relaxation experiment, a ring specimen was held at a constant stretch ratio, and the lifetime of the specimen was measured. The apparatus for the lifetime measurement is the same that is shown in the previous paper.[19] The measurements at various stretch ratios were performed on 20 specimens. The stress relaxation property of SBS was also studied.

TEM Observation of Microstructure

The microstructure of SBS both in an unstretched state and in stretched states were observed by TEM. For the observation, the ring specimen stretched

by a constant stretch ratio was fixed to a metal frame, and was stained in osmium tetroxide vapor for 48 h at room temperature. The stained specimens were cut into a ribbon shape, and were embedded in epoxy resin. Ultrathin sections were made by cutting the embedded specimens frozen in liquid N_2 parallel to the stretching direction.

Pulsed NMR Measurements

Pulsed NMR measurements were performed with JEOL-FSE-60Q spectrometer operating at 60 MHz for protons (^1H) in the phase-sensitive detection mode. The recovery time of the spectrometer following a sequence of pulses was about 10 μs and 90° pulse was of 2 μs duration. The NMR signal was fed into a transient recorder with a signal averager (Model KR 3160, Kawasaki Electronica Co., Ltd.) and was stored in memory. Then, the digitized data on the NMR signal were transferred to a microcomputer (Model PC 9801F, NEC, Ltd.) and were analyzed by the least squares method. The temperature of the specimen was controlled by flowing cold air passing through liquid N_2 and an electrical heater.

The pulse sequences for T_2 measurements were the solid echo pulse sequence $(90_x^\circ\tau 90_y^\circ)$[31] available for short T_2 component to avoid the effect of the dead time after the pulse and Carr–Purcell–Meiboom–Gill (CPMG) pulse sequence $[90_x^\circ\tau(180_y^\circ 2\tau)_n]$ $(n = 3000)$[32,33] available for long T_2 component to eliminate the effect of inhomogeneity in the static magnetic field. Especially in the solid echo pulse sequence, the value of τ was adjusted properly in order to attain the maximum intensity of the decay signal without the effect of the dead time of the spectrometer. By the above method of the T_2 measurement, the T_2 signal for the mechanically blended incompatible polymer system,

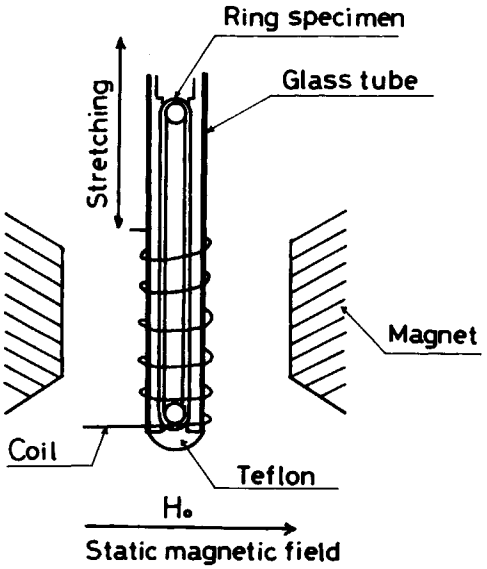

Fig. 1. Schematic illustration of T_2 measurement in a stretched state for SBS. A ring specimen is held at a constant stretch ratio and the stretching direction is selected to be perpendicular to the static magnetic field.

which is composed of rubbery and glassy components, was analyzed as the sum of the Gaussian component and exponential one. It is convinced that the T_2 signal for each component evaluated is proportional to the fraction of protons for the component accurately.[34] After Tanaka and Nishi,[30] the signals obtained from both the pulse sequences were combined at a time (150 ~ 200 μs), before dephasing due to inhomogeneity in the magnetic field becomes important. Figure 1 shows the schematic illustration of the T_2 measurement in a stretched state for SBS. A ring specimen of SBS was held at a constant stretch ratio. The stretching direction was selected to be perpendicular to the static magnetic field.

The spin-lattice relaxation time T_1 for SBS was measured by the modified inversion recovery pulse sequence $(180_x^\circ \tau 90_x^\circ \tau_0 90_y^\circ)$[26] utilizing the solid echo pulse sequence to avoid the influence of the dead time. The spin-lattice relaxation time in the rotating frame, $T_{1\rho}$, for SBS was measured by the solid echo train pulse sequence $[90_x^\circ \tau (90_y^\circ 2\tau)_n]$ $(n = 3000)$.[35]

RESULTS

Tensile Property and Failure Behavior in Stress Relaxation

Figure 2 shows the tensile stress–strain curve of SBS as compared with the typical curves of unfilled and filled crosslinked rubbers with carbon black particles. It is found that the stress–strain curve of SBS is analogous to that of the unfilled rubber at small deformation and to that of the filled rubber at large deformation, in which the stress rises steeply against the strain.

A statistical analysis of the distribution of the lifetime in the stress relaxation process was made by using Weibull function[36] on the basis of the stochastic theory for the failure of crosslinked rubbers proposed by Kawabata[37] and Fukumori and Kurauchi.[19] In the theory, the probability of survival, $R(t)$, is expressed by

$$R(t) = \exp\left[-(t/\beta)^m\right] \tag{1}$$

where t is time and m and β are constants. From eq. (1), the mean lifetime

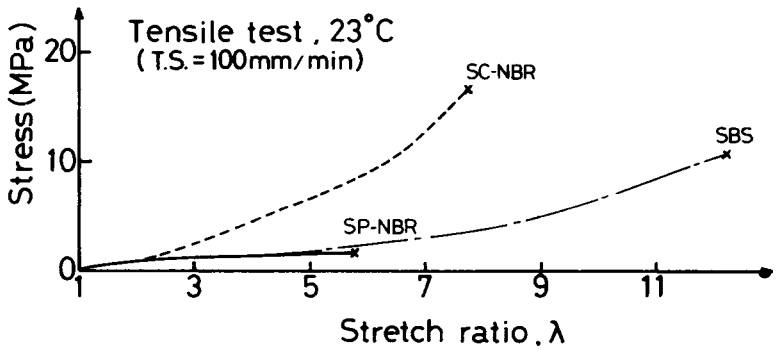

Fig. 2. Stress–strain curve of SBS as compared with the typical curves of the crosslinked rubbers: (unfilled) SP–NBR; (filled) SC–NBR.

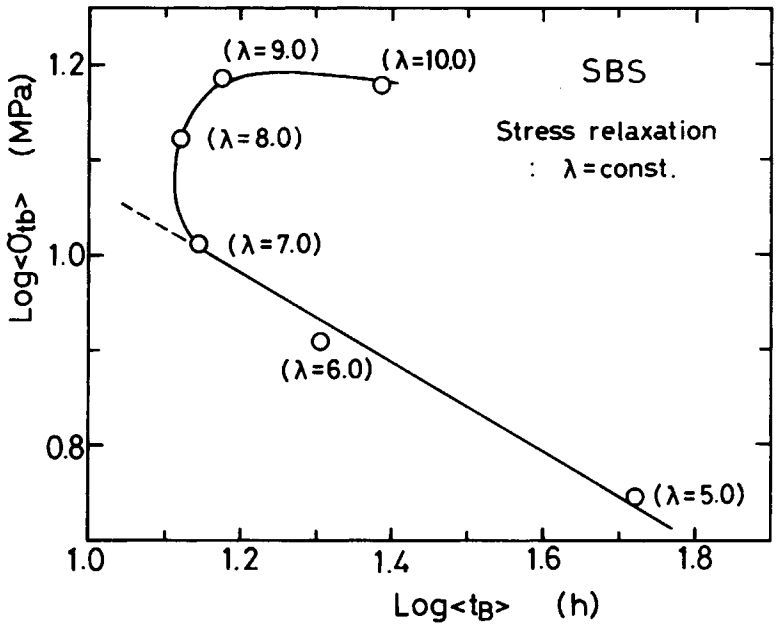

Fig. 3. Plot of $\log\langle\sigma_{tb}\rangle$ against $\log\langle t_B\rangle$ for SBS in stress relaxation.

$\langle t_B\rangle$ is obtained as

$$\langle t_B\rangle = \beta \cdot \Gamma(1 + 1/m) \tag{2}$$

where Γ is the gamma function.

Figure 3 shows the dependence of the mean lifetime $\langle t_B\rangle$ on the mean breaking true stress $\langle\sigma_{tb}\rangle$ in the stress relaxation experiments. In this figure, on the basis of the stochastic theory, $\log\langle\sigma_{tb}\rangle$ is plotted against $\log\langle t_B\rangle$. The plot makes a straight line in the range up to the stretch ratio λ of 7.0 in accordance with the results for the crosslinked rubbers. The plot at the higher stretch ratio than 7.0 deviates strongly from the linear relationship. It is found that the mean lifetimes at λ of 7.0, 8.0, and 9.0 are almost the same and that the mean lifetime at λ of 10.0 is longer than those at lower stretch ratios. In the stress relaxation process, the stress $\sigma(t)$ is empirically given by the following equation[19,37]:

$$\sigma(t) = A \cdot t^{-k_r} \tag{3}$$

where A and k_r are constants and k_r is the stress relaxation rate. The values of k_r are plotted against $\log\langle t_B\rangle$ in Figure 4. The stress relaxation behavior of SBS at the lower stretch ratio up to 7.0 is analogous to that of the carbon-filled rubber, for which the mean lifetime decreases with the increase of k_r. At the higher stretch ratio than 7.0, the value of k_r for SBS increases remarkably, which reflects the difference between the stress relaxation behavior of SBS and that of the carbon-filled rubber.

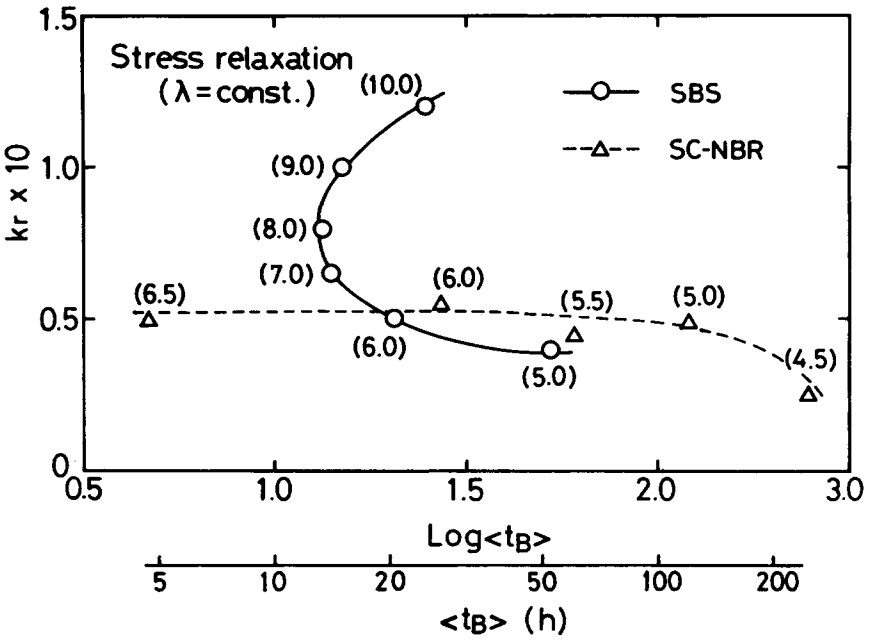

Fig. 4. Stress relaxation rate k_r plotted against $\langle t_B \rangle$ for SBS and crosslinked rubber filled with carbon black particles (SC-NBR). Numerical values corresponding to those of stretch ratios.

Thus, it is believed that different stress relaxation mechanism from that in the crosslinked rubbers may be involved in releasing of stress concentration in SBS and increasing of the lifetime of the material.

Change of Microstructure on Deformation

Figure 5 shows TEM photographs of ultrathin sections of SBS specimens in unstretched and stretched states. As shown in Figure 5(a), SBS as molded by compression molding in the unstretched state has heterogeneous structure, in which PS domains (PS spheres interconnected to form a swivel-like structure) are uniformly dispersed in continuous PB matrix. As shown in Figure 5(b), at λ of 7.0, the PS domains come to be aligned in the stretching direction associated with the deformation of the PB chains, which may be involved with the overall deformation of the system. At λ of 9.0 [Fig. 5(c)], the PS domains are oriented in the stretching direction and become more ellipsoidal, which may reflect that the PB chains become fully extended. At λ of 10.0 [Fig. 5(d)], the interconnected PS spheres come to be separated to be individual particles, and the rearrangement of the PS domains occurs.

Thus, it can be suggested that considerable dissipation of the strain energy stored through stretching may be caused by the disruption of interconnections between the PS spheres, giving rise to the remarkable increase of the value of k_r.

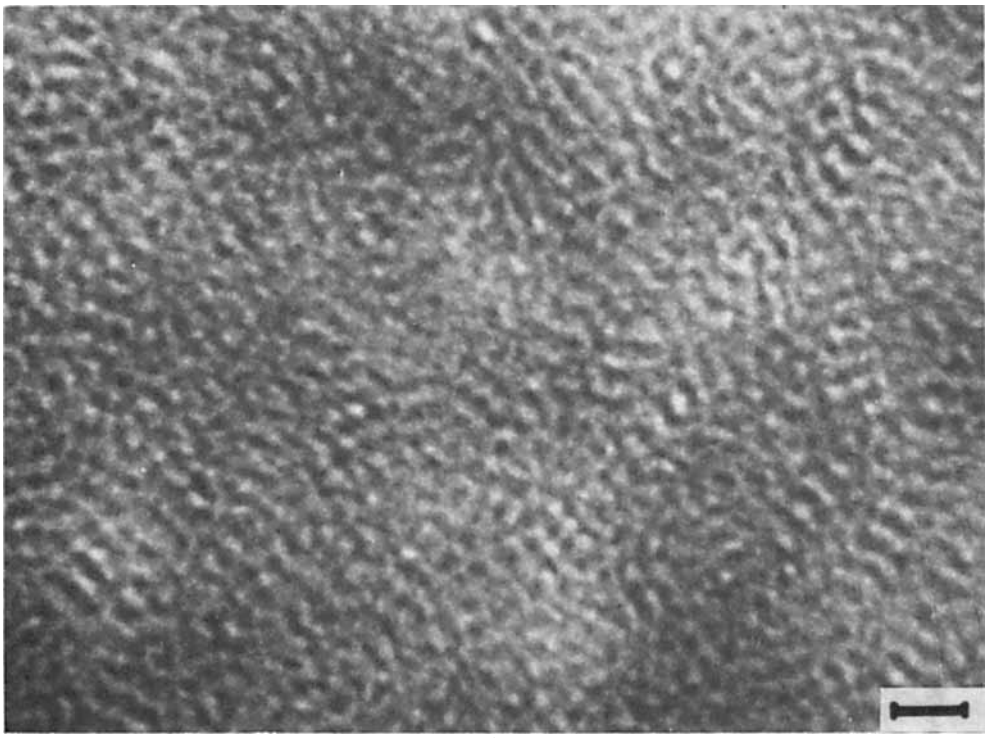

(a)

Fig. 5. TEM photographs of SBS specimens: (a) unstretched; (b) stretched to $\lambda = 7.0$; (c) stretched to $\lambda = 9.0$; (d) stretched to $\lambda = 10.0$. Arrows indicate the stretching direction. The bars corresponding to 100 nm. The dark stained region is PB component.

Molecular Mobility of SBS in the Stretched State

Generally, the transverse magnetization decay signal (T_2 signal), $M(t)$, for solid polymers is expressed as a function of the correlation time of molecular motion, τ_c, by the following[38,39]:

$$M(t) = M_0 \exp\{-\sigma_0^2 \tau_c^2 [\exp(-t/\tau_c) + t/\tau_c - 1]\} \tag{4}$$

where M_0 is a constant proportional to the total number of nuclei with magnetic moment and σ_0^2 the second moment in the rigid lattice.[40] σ_0^2, which reflects the interaction among nuclear spins, is given by

$$\sigma_0^2 = (6/5)I(I+1)g^2\mu_N^2 N^{-1} \sum_i \sum_j \langle r_{ij}^{-6} \rangle \tag{5}$$

where I is the spin of the nucleus with magnetic moment ($I = 1/2$ for ^1H), g the g factor, μ_N the nuclear magnetization, N the total number of nuclei with

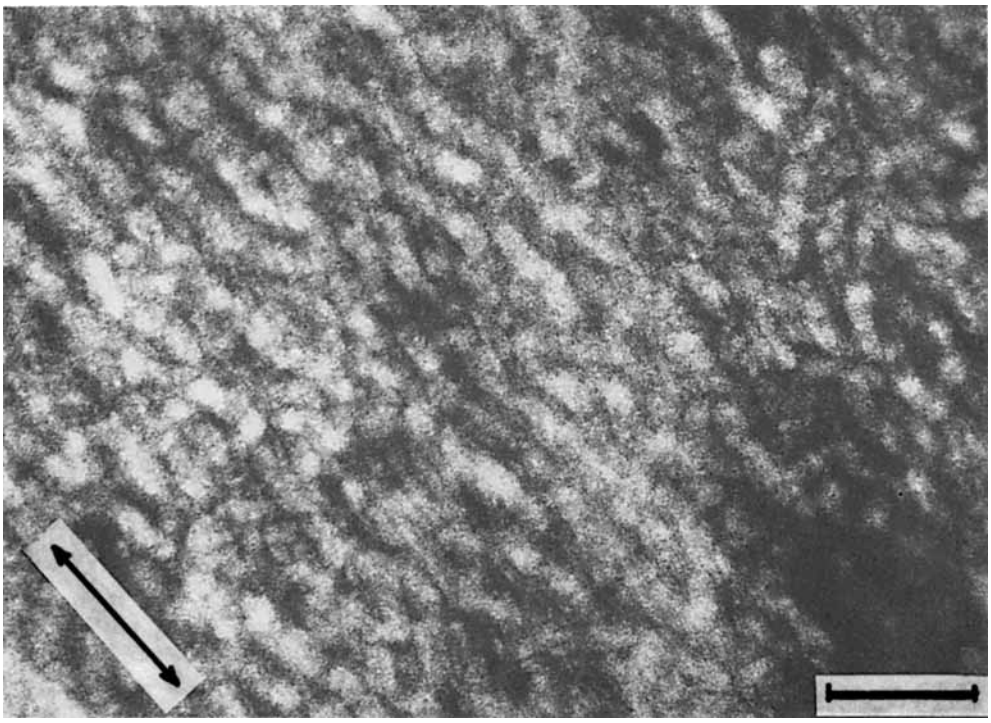

(b)

Fig. 5. *(Continued from the previous page.)*

magnetic moment, and r_{ij} the distance between nuclei i and j. For $\tau_c\sigma_0 \ll 1$,

$$M(t) = M_0 \exp(-t/T_2) \tag{6}$$

$$T_2 \sim \left(\sigma_0^2 \tau_c\right)^{-1} \tag{7}$$

For $\tau_c\sigma_0 \gg 1$,

$$M(t) = M_0 \exp\left[-\tfrac{1}{2}(t/T_2)^2\right] \tag{8}$$

$$T_2 \sim \sigma_0^{-1} \tag{9}$$

In the intermediate condition, $M(t)$ is expressed empirically as following Weibull function[41,42]:

$$M(t) = M_0 \exp\left[-(1/a)(t/T_2)^a\right] \tag{10}$$

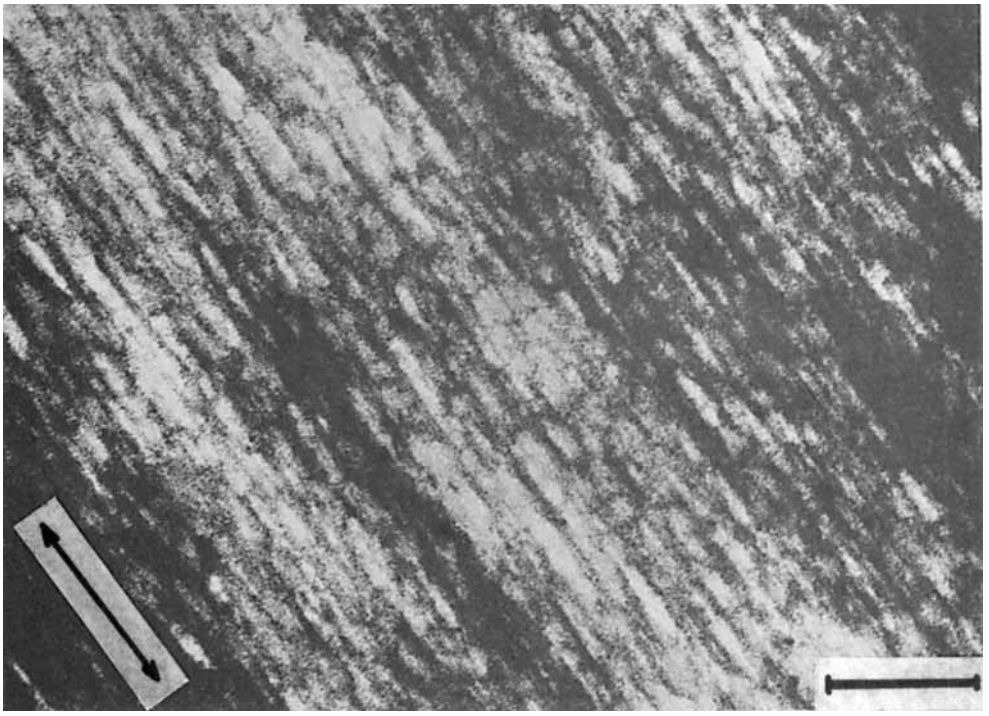

(c)

Fig. 5. (*Continued from the previous page.*)

where a is the shape parameter. Hence, in the T_2 measurement, the change of T_2 should be related to both the changes of τ_c and σ_0^2 based on the microscopic foundation. The molecular mobility of the polymer chains strongly depends on the flexibility of polymers, the tension on the polymer chains, and the degree of orientation of molecules. The degree of orientation is also connected with σ_0^2. The appearance of the highly ordered structure is attributed to the increase of σ_0^2, i.e., the decrease of T_2.

On deformation, τ_c and σ_0^2 are considered to depend on the stretch ratio λ, which causes T_2 to depend on λ. Considering both the intramolecular and intermolecular contributions to the second moment, $\sigma_0^2(\lambda)$ calculated for crystallizable crosslinked natural rubber (NR) is not much affected by the stretch ratio λ [$\sigma_0^2(1) = 18.8$ (gauss)^2 and $\sigma_0^2(5) = 18.6$ (gauss)^2, respectively] under the condition that the strain-induced crystallization does not occur.[43] Furthermore, it was reported that the dependence of T_2 for NR on the stretching direction in the static magnetic field is negligible, indicating that the effect of the anisotropy induced by the stretching of the rubber is hardly affected by T_2 with this method.[44] Thus, it can be expected for chemically or physically crosslinked elastomers that T_2 depends on the stretch ratio mainly through the dependence of the correlation time of molecular motion in the rubbery phase if strain-induced crystallization does not occur. In this study, on the basis of eqs. (4)–(10), the T_2 signals for SBS, which is noncrystallizable, were analyzed by nonlinear least square method.

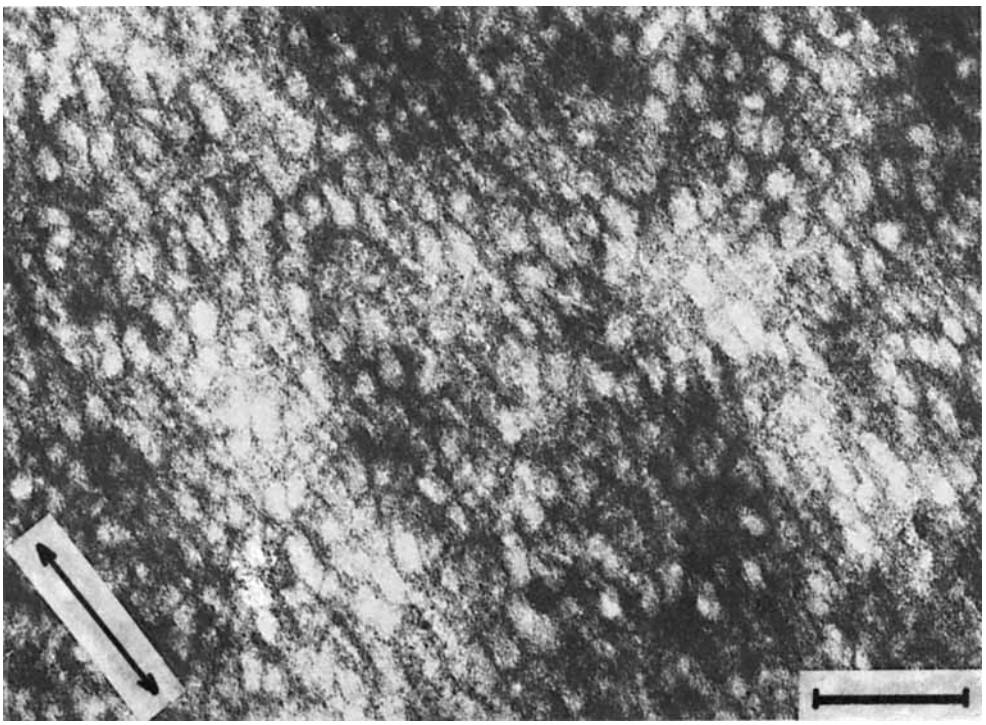

(d)

Fig. 5. (*Continued from the previous page.*)

Figure 6 shows the result of the T_2 measurement with SBS in an unstretched state. The T_2 signal for SBS in the unstretched state is resolved into three components, fitted by the sum of Gaussian (short) and two exponential (medium and long) decay functions. As already mentioned, SBS used in this study contains the naphthenic oil as plasticizer which is readily dissolved in the rubbery phase. Proton fractions of PS component and PB component containing the naphthenic oil in SBS compound are about 20 and 80%, respectively. Hence, the short T_2 component (ca. 14% proton fraction) is assigned to the PS component, and the medium and long T_2 components to the PB component having some heterogeneous structure, partially dissolved with PS chains (ca. 6% proton fraction).

Figure 7 shows the result of the $T_{1\rho}$ measurement with SBS in the unstretched state. The $T_{1\rho}$ signal can be resolved into three components, analyzed by the sum of the exponential decay functions. Figure 8 shows the result of the T_1 measurement with SBS in the unstretched state. The T_1 signal for SBS is composed of one component, in which the information on the spatial inhomogeneity in SBS may be lost through the spin diffusion process. The results obtained from the T_2, $T_{1\rho}$, and T_1 measurements are summarized in Table I.

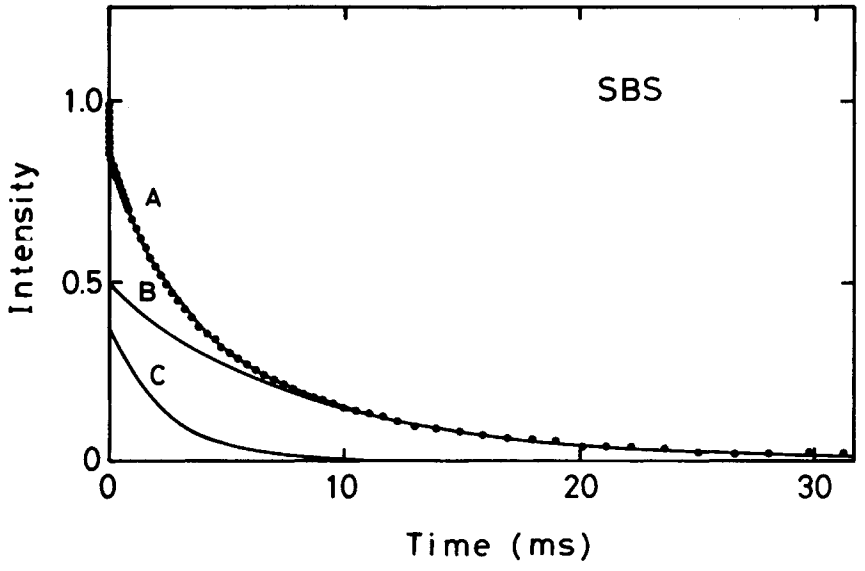

(a)

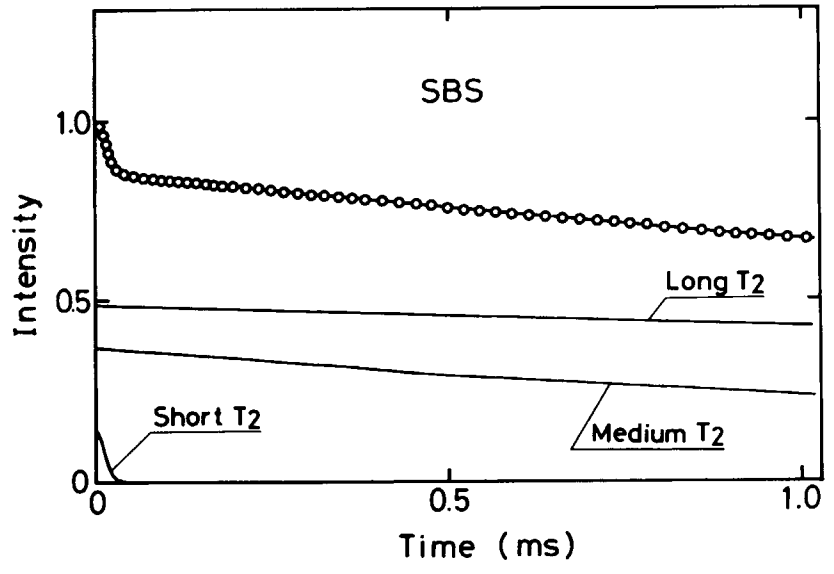

(b)

Fig. 6. T_2 signal for SBS in an unstretched state: (a) The solid line A is the calculated curve on the basis of eqs. (6)–(10) by nonlinear least square method. The solid lines B and C represent the exponentially decaying components. (b) Short time behavior of T_2 signal resolved into three (short, medium, and long) T_2 components.

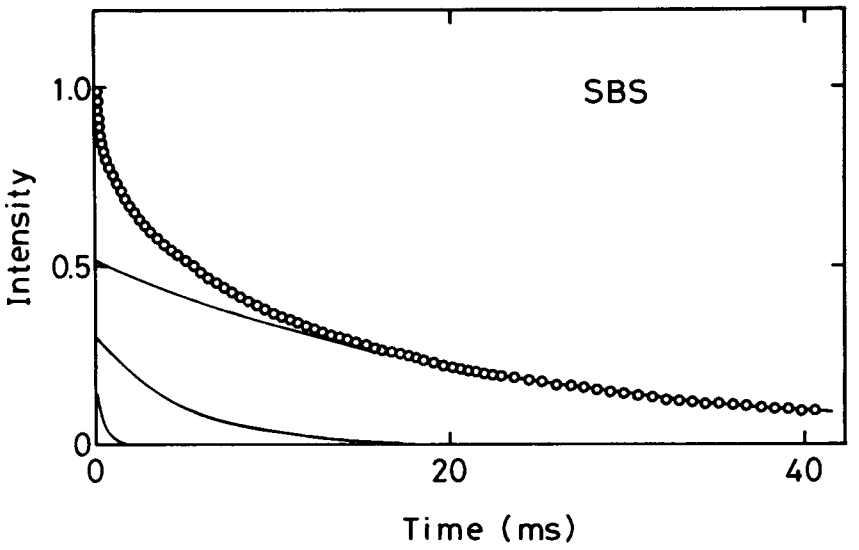

Fig. 7. $T_{1\rho}$ signal for SBS in an unstretched state. The signal composed of three exponentially decaying component signals.

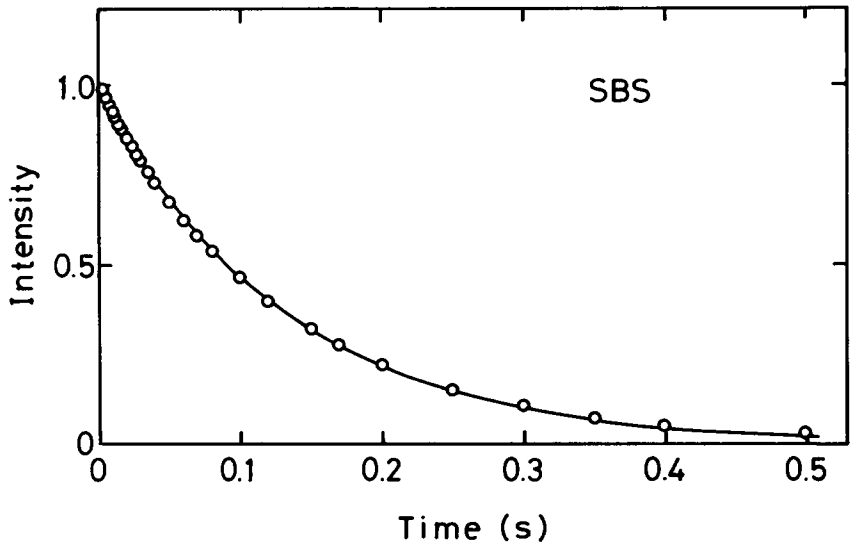

Fig. 8. T_1 signal for SBS in an unstretched state. The signal is composed of one exponentially decaying component signal. Time in the figure corresponding to pulse interval τ.

Figures 9 and 10 show the results of the T_2 measurements with SBS specimens at λ of 3.0 and 10.0, respectively. The T_2 signal decays more rapidly with the increase of the stretch ratio in comparison with the result in the unstretched state shown in Figure 6. Moreover, the T_2 signals in the stretched states can be apparently resolved into four components, which may reflect that the heterogeneity in the structure increases with stretching, fitted by the sum of Gaussian (short), Weibull [medium (S)], and two exponential [medium (L) and long] decay functions.

TABLE I
Results of T_2, $T_{1\rho}$, and T_1 Measurements with SBS in an Unstretched State
(Fraction Amounts and Relaxation Time)

$T_2(s)$			$T_{1\rho}(s)$			$T_1(s)$
$T_2(1)$	$T_2(2)$	$T_2(3)$	$T_{1\rho}(1)$	$T_{1\rho}(2)$	$T_{1\rho}(3)$	$T_1(1)$
14%	37%	49%	19%	30%	51%	100%
1.3×10^{-5}	2.3×10^{-3}	8.2×10^{-3}	4.4×10^{-4}	4.8×10^{-3}	2.3×10^{-2}	1.3×10^{-1}

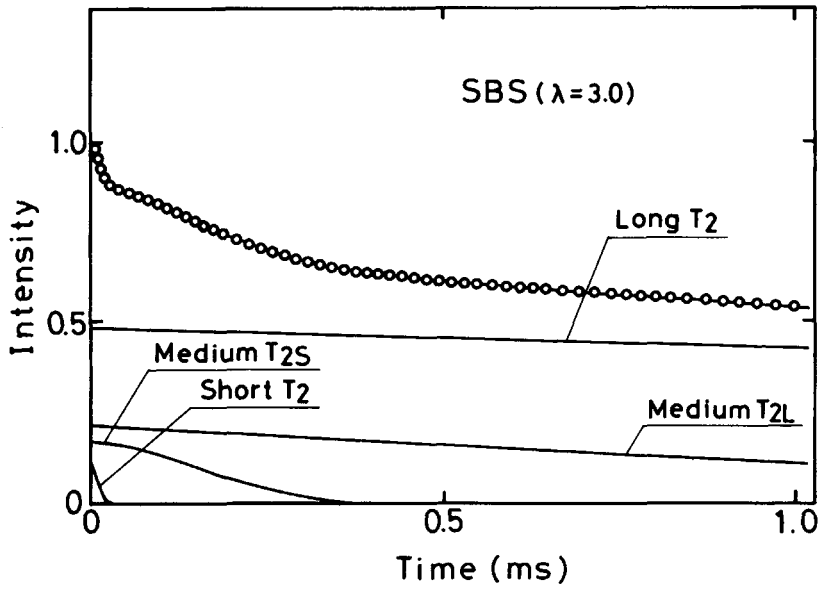

Fig. 9. T_2 signal for SBS at stretch ratio λ of 3.0 in similar time range to that shown in Figure 6(b). Medium T_2 component was separated into two components (T_{2S} and T_{2L}).

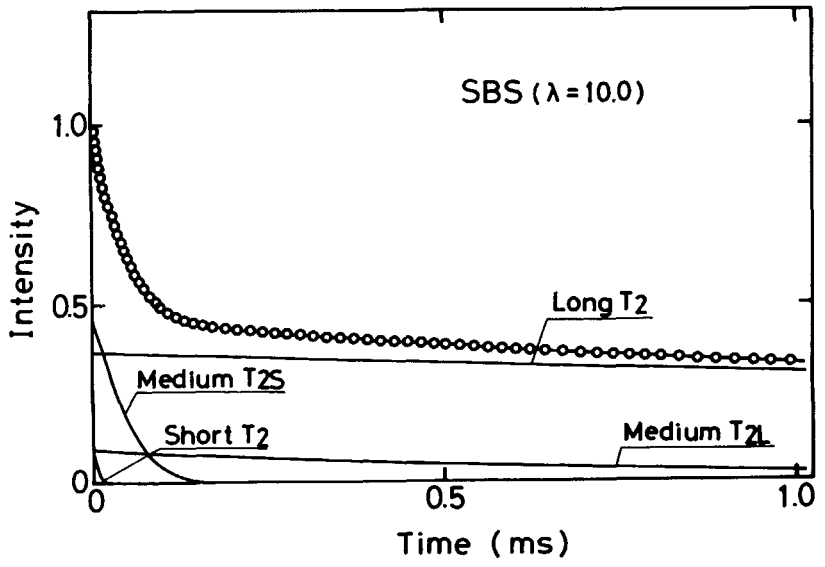

Fig. 10. T_2 signal for SBS at stretch ratio λ of 10.0 in similar time range to that shown in Figure 6(b).

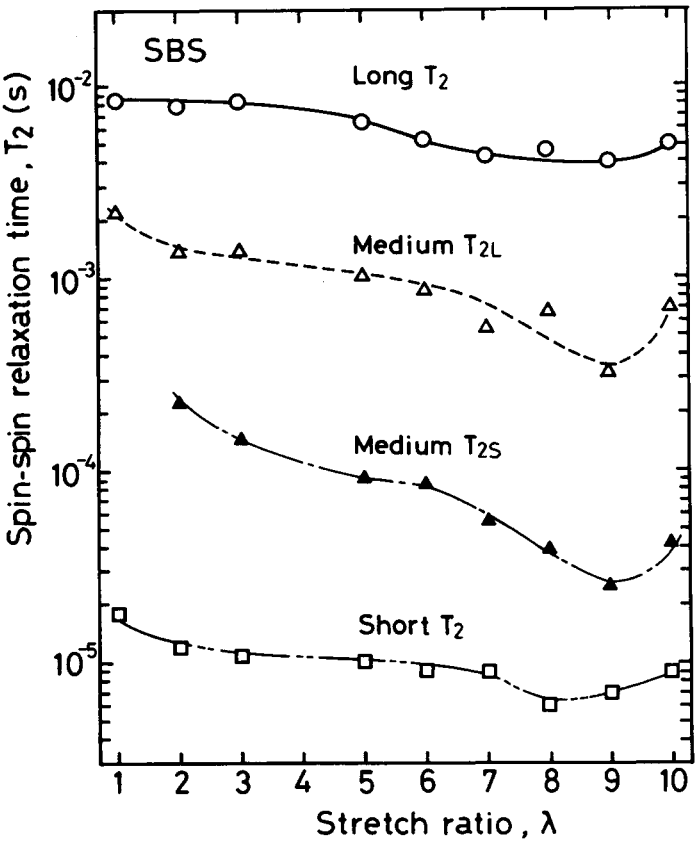

Fig. 11. Dependence of the values of the T_2 components on λ for SBS. In stretched states, the T_2 signal was resolved into four T_2 components.

Figure 11 shows the dependence of the values of the T_2 components for SBS on the stretch ratio λ. In the unstretched state, three T_2 components (short T_2, medium T_2, long T_2) are observed. With stretching, it is found that the medium T_2 is separated into two components (medium T_{2S} and T_{2L}), and that medium T_{2S}, medium T_{2L}, and long T_2 become shorter, which implies the increase of the restriction of the molecular motion of the polymer chains corresponding to these T_2 components. Especially, the medium T_{2S} becomes shorter with stretching and the molecular mobility of the medium T_{2S} component gradually approaches to that in the glassy state ($T_2 \sim 10$ μs). However, all the T_2 components at λ of 10.0 become a little longer than those at λ of 9.0. The increases of all the values of the T_2 components reflect some release of the constrained molecular mobility of the overall polymer chains in SBS. The appearance of the medium T_{2S} component fitted by the Weibull function shows that the degree of motional vigor attained by molecules in the corresponding region is intermediate between the near liquidlike character of the rubbery molecules and the more restricted motions in the glassy domain (i.e., a limited constraint on the motions ultimately achieved).

Figure 12 shows the change of the fraction (proton %) of each T_2 component with stretching. The fraction of the medium T_{2S} component increases remarkably at the higher stretch ratio, in which the increase in the fraction of the

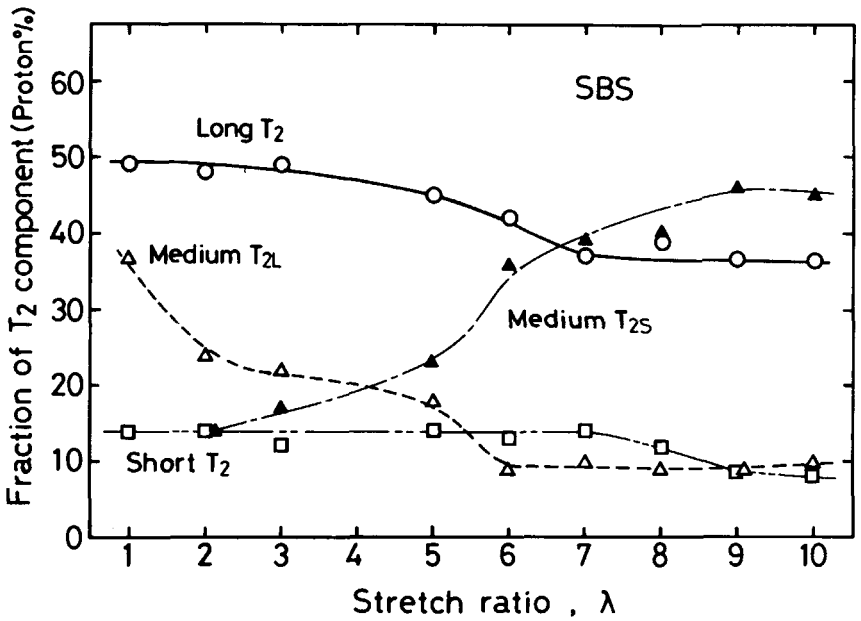

Fig. 12. Dependence of the fraction of the T_2 components (proton %) on λ.

medium T_{2S} component comes from the decreases in the fractions of other T_2 components, especially from medium T_{2L} component.

From these results, it is considered that the molecular motion of the polymer chains in PB phase corresponding to the medium T_2 component becomes strongly constrained with the increase of the stretch ratio and that the restriction for the region is partially released in the higher stretched state over the critical value. This critical value ($\lambda = 10.0$) is identical with that obtained from both the stress relaxation experiments and TEM observation of the microstructure.

DISCUSSIONS

Heterogeneity in SBS

In this study, the T_2 signal without the influence of the spin diffusion for SBS in the unstretched state is composed of three components (short, medium, and long), and in the $T_{1\rho}$ and T_1 measurements, in which the spin diffusion is relatively effective. In the spin diffusion process, the maximum diffusive path length L is approximately expressed by the equation as

$$L \sim (6D\tau_{SD})^{1/2} \tag{11}$$

where D is the spin diffusion coefficient and τ_{SD} is the characteristic time for diffusion.[22-25] Hence, the observation of the time required for internal equilibration of the motionally heterogeneous regions in a spin system provides a measure of the dimension involved in the transport process of the spin energy,

when the spin diffusion coefficient is known (typically, of the order of 10^{-12} cm^2 s^{-1}). In the T_1 and $T_{1\rho}$ measurements, in which T_1 and $T_{1\rho}$ minima are generally in the respective time domains of about 10^{-1} and 10^{-3} s, an efficient relaxing region can relax neighboring nuclei within a range of the orders of 10 and 1 nm, respectively.

Thus, from the results of the $T_{1\rho}$ and T_1 measurements shown in Figures 7 and 8, the spatial inhomogeneity in SBS specimen can be approximately estimated to be of the order of 10 nm, because the information on the heterogeneous structure in SBS is lost in the T_1 measurement (one component observed) and the spin diffusion is relatively ineffective for more remote nuclei than the diffusive path length in the $T_{1\rho}$ measurement (three components observed).

According to Tanaka and Nishi,[26,30] in the T_2, $T_{1\rho}$, and T_1 measurements for styrene–diene triblock copolymers containing no plasticizer, the numbers of the components are three, two, and one, respectively, and they suggested that the origin of the medium T_2 component may be the interface of the two phases, because the information about the spatial inhomogeneity (of the order of 1 nm) in the block copolymers is lost in the $T_{1\rho}$ measurements.

SBS added with the plasticizer for the engineering practice used in this study may have less regular structure than the block copolymers containing no plasticizer. In addition, hot milling and molding processes may cause some disruption of the domain structure and some remixing of the phases, associated with different structures from those made by solvent castings.[9,10,45] The diffuseness and thickness of the phase boundaries in the block copolymers depend on the nature of the blocks and solidification conditions. It is found that the phase boundaries in the compression-molded SBS are very diffuse and the dark stained PB phase has a mottle appearance as shown in Figure 5, indicating the presence of some PS chains mixed. In the T_2 measurements, the motional heterogeneity in PB phase observed is probably due to the intermolecular contributions related to the state of the mixing of the PB chains and plasticizer, i.e., assigned to the oil-poor PB phase and oil-rich one. From the results of the T_2, $T_{1\rho}$ and T_1 measurements, it is believed that the medium T_2 component is assigned to oil-poor PB phase, which has almost similar molecular mobility to the T_2 component for PB phase containing no plasticizer[27] and is partially mixed with PS chains, and short and long T_2 components to PS phase and oil-rich PB phase, respectively. Similar results of the pulsed NMR measurements with the heterogeneous structure in the plasticized poly(vinyl chloride) (PVC), which is composed of unplasticized PVC phase and plasticized PVC phase, were reported.[24,25] Hence, because of the complicated heterogeneity in PB phase, in which the spatial heterogeneity is of the order of more than 1 nm, the interface layer between PS and PB phases in SBS examined may be obscured.

From all the results of the stress relaxation experiments, TEM observations and T_2 measurements with SBS, it can be confirmed that the high energy dissipation in SBS occurs at the stretch ratio of 10.0 and is caused by the disruption of the interconnections between the PS spheres, which is closely related to the remarkable increase of the value of k_r and the increase of the molecular mobility in SBS, associated with the increase of the lifetime of the material in the stress relaxation process.

Deformation Mechanism of SBS

In the T_2 measurements for crosslinked nitrile–butadiene copolymer rubbers (NBR), two T_2 (short and long) components were observed, concerned with some heterogeneity in the molecular mobility of the network chains. The short T_2 component becomes shorter and its fraction increases with stretching. Hence, it was suggested that the short T_2 component is assigned to the regions of the network chains in constrained conformations in the vicinity of the crosslinking points.[46] Figure 13 shows the schematic illustrations of the motional heterogeneity in the crosslinked rubbers under deformation. It is shown in the figure that the constrained regions of the network chains under the influence of the crosslinks may be enlarged with stretching corresponding to the increase of the fraction of the short T_2 component.

In ^{2}H-NMR studies on strained selectively deuterated elastomers,[21] it was shown that the orientation of the chain molecules attached to crosslinks (deuterated networks selectively at crosslinks) is larger than the average molecular orientation in a crosslinked 1.4-butadiene rubber, which may be consistent with the above-mentioned results for NBR obtained from the T_2 measurements. In the T_2 measurements of the block copolymers, the relaxation process in the phase boundaries seems to be mainly due to the intramolecular interactions, which is related to the restriction of the molecular motion caused by the connectivity of the rubbery segments to the hard domains with low mobility. In qualitative discussion of the constrained motion for the bound part of fold and cilia in semicrystalline polymers by Douglass et al.,[47] T_2 for each element takes the form

$$T_2^2 = \exp(3N_0\alpha^2)T_{2\mathrm{RL}}^2 \tag{12}$$

where N_0 is the number of the element, α the typical bend angle, and $T_{2\mathrm{RL}}$ the intra rigid lattice T_2. In the above expression, the flexibility of the segments

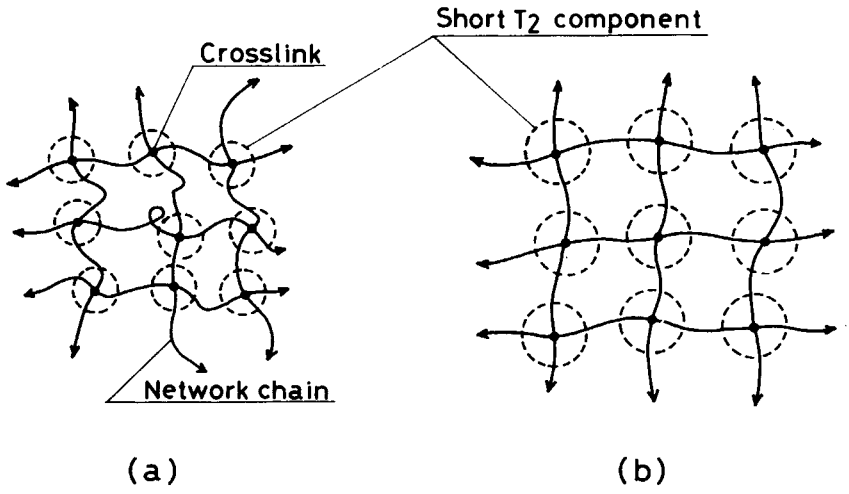

Fig. 13. Schematic illustrations of the motional heterogeneity in the crosslinked rubbers under deformation: (a) unstretched; (b) stretched.

may remarkably decrease as the bend angle α or the number of elements N_0 decreases, and the line width decreases progressively as one proceeds away from the point of constraint. Therefore, from eq. (12), the constrained anisotropic motions of the rubbery chains in the stretched states, which closely depend on the contour length from the hard domains, can be qualitatively estimated in some degrees.

In the T_2 measurements for SBS, three T_2 (short, medium, and long) components are observed in the unstretched state, and the medium component is resolved into two components (T_{2S} and T_{2L}) on deformation. The medium T_{2S} component for SBS becomes shorter and its fraction increases remarkably with stretching in similar manner to the short T_2 component for NBR. These behaviors of the medium T_{2S} component in the stretched states may reflect the changes of the molecular state and spatial distribution of the motionally constrained PB chains under the influence of the PS domains. Hence, it is believed that the changes of the fractions of the medium and long T_2 components may be concerned with the change of the spatial distribution of τ_c along the PB chains under deformation through the intramolecular interactions, as schematically shown in Figure 14. In this study for SBS, it is probable that some spatially averaged molecular mobility of corresponding PB chains in the stretched states may be estimated in the static magnetic field by the T_2 measurements. In the rubbery polymers in which intermolecular forces are small, the stress transfer occurs through the entropy-elastic deformation of the network chains. Therefore, the limited extensibility of the polymer chains between adjacent points of attachment (crosslink or filler particle) and the mechanisms of the network rupture have to be discussed for the rubbery polymers. For SBS, it is suggested that the fraction of the medium T_{2S} component amounts to the maximum at $\lambda = 9.0$ through the limited extensibility of the PB chains between the adjacent PS domains attained. At the critical strain ($\lambda = 10.0$), all the values of the T_2 components

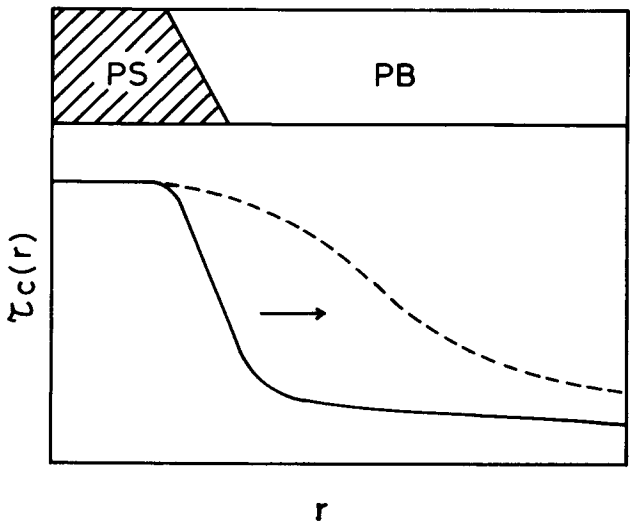

Fig. 14. Spatial profile of the correlation time of the molecular motion τ_c in SBS is shown schematically as a function of r: (—) unstretched; (---) stretched.

increase, which may be connected with the stress relief for the overall polymer chains in SBS caused by the disruption of the weak interconnections between the spherical domains. However, the fraction of the medium T_{2S} component hardly changes at the critical strain, reflecting that the fraction of the constrained regions under the influence of the PS domains may be retained. In contrast with SBS (physically crosslinked), various mechanisms of the occurrence of the network rupture for the chemically crosslinked rubbers are conceivable such as the chain scissions, breakage of crosslinks or filler–rubber bondings, and so on. Detailed analysis for the crosslinked rubbers will be presented in the near future. In addition, for some decrease of the fraction of the short T_2 component at $\lambda > 7.0$, it is probable that this behavior may correspond to the structural change of some part of the PS domains (not drastic as that at the critical strain) on deformation ($\lambda = 8.0$–9.0) with some energy dissipation, consistent with the results that the mean lifetime at λ of 7.0, 8.0, and 9.0 in the stress relaxation experiments are almost the same.

Figure 15 shows the schematic illustrations of the deformation mechanism for SBS. In the initial state, short swivel-like PS domains are randomly dispersed in the rubbery PB matrix. With stretching, the alignment, orientation, and deformation of the PS domains occur in the stretching direction, and it is related to the deformation and orientation of PB chains causing the restriction of the molecular motion of those near the PS domains. At the critical level ($\lambda = 10.0$), the interconnections between the spherical PS domains disappear, in which the lower energy consumption for the disruption of the weak interconnections may be met sooner than the higher energy consumption for scission of PB chains. On the other hand, the localized heterogeneous structure in PB phase caused by the deformation is not recovered, in which microvoids occur and ultimately grow to form cracks.

In the stress relaxation process, the true stress decreases monotonically with time at a constant stretch ratio. The high energy dissipation associated with the change of the microstructure in SBS at the large deformation is involved in relieving the local stress concentrations and leading the material to be more

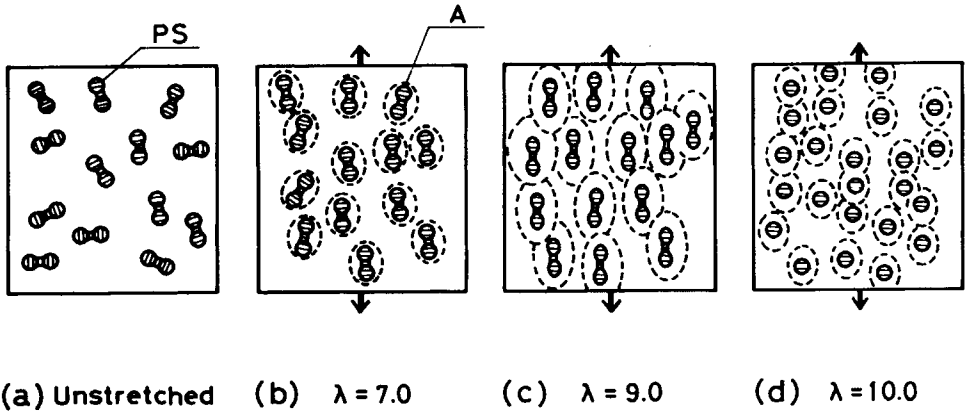

Fig. 15. Schematic illustrations of the changes of the microstructure in SBS on deformation. A regions represent the polymer chains in PB phase in constrained conformations around the PS domains, corresponding to the medium T_{2S} component in the T_2 measurements.

stabilized against the failure as long as the strain is held constant. Dangling fragmented PS domains in PB phase may be regarded as relatively stable to the initiation of a critical crack in the stress relaxation process compared with the PS domains in the creep process and simple tensile process.

CONCLUSIONS

A pulsed NMR study of an elastomeric block copolymer (SBS) under deformation was done in order to understand the deformation behavior of the network chains between adjacent points of attachment (crosslink or filler particle) in crosslinked rubbers. In the stress relaxation process at the critical strain, the mean lifetime of SBS becomes longer than that at lower strain in contrast with the results for the crosslinked rubbers. This behavior cannot be understood by the results of simple mechanical experiments. By the T_2 measurements, it was suggested for SBS that the PB chains in the vicinity of the PS domains come to be in more constrained conformations than those remote from the domains under deformation, associated with the roles of the crosslinks and filler particles, and that the constrained regions under the influence of the domains are enlarged with stretching. It is believed that the disruption of the weak interconnections between the spherical PS domains observed by TEM occurs at the critical strain through the limited extensibility of the PB chains attained and leads the material to be more stabilized against the failure with high energy dissipation, related to the enhancement of the molecular mobility of the overall polymer chains in SBS.

In this study, it becomes clear that the results obtained by the pulsed NMR measurements complement the mechanical measurements and TEM observations with a more precise identification of the mobile, or immobile, entities assigned to the small scale heterogeneity in SBS. Hence, it can be expected that this method may provide useful information on the motional heterogeneity in the crosslinked rubbers under deformation, for which the contrast between the components may be insufficient for other methods such as TEM and SAXS, because of the lack of a suitable staining method or enough discrepancies in the electron density.

The authors are indebted to Professor T. Nishi and Dr. H. Tanaka, Department of Applied Physics, Faculty of Engineering, University of Tokyo, for their valuable suggestions in the pulsed NMR measurements. They also thank Mr. N. Suzuki for taking the TEM photographs of the specimens.

References

1. L. R. G. Treloar, *The Physics of Rubber Elasticity*, 3rd ed., Clarendon, Oxford, 1975.
2. J. A. Manson and L. H. Sperling, *Polymer Blends and Composites*, Plenum, New York, 1976, p. 121.
3. J. C. West and S. L. Cooper, in *Science and Technology of Rubber*, F. R. Eirich, Ed., Academic, New York, 1978, p. 531.
4. D. M. Brunwin, E. Fischer, and J. F. Henderson, *J. Polym. Sci. Part C*, **26**, 135 (1969).
5. D. G. Fesko and N. W. Tschoegl, *J. Polym. Sci. Part C*, **35**, 51 (1971).
6. D. H. Kaelble, *Trans. Soc. Rheol.*, **15**, 235 (1971).
7. D. H. Kaelble and E. H. Cirlin, *J. Polym. Sci. Symp.*, **43**, 131 (1973).
8. M. Shen and V. A. Kaniskin, *J. Polym. Sci., Polym. Phys. Ed.*, **11**, 2261 (1973).
9. J. A. Odell and A. Keller, *Polym. Eng. Sci.*, **17**, 544 (1977).

10. J. F. Beecher, L. Marker, R. D. Bradford, and S. L. Aggarwal, *J. Polym. Sci. Part C*, **26**, 117 (1969).
11. T. L. Smith and R. A. Dickie, *J. Polym. Sci. Part C*, **26**, 163 (1969).
12. T. L. Smith, in *Block Polymers*, S. L. Aggarwal, Ed., Plenum, New York, 1970, p. 137.
13. T. L. Smith, *J. Polym. Sci., Polym. Phys. Ed.*, **12**, 1825 (1974).
14. T. Inoue, M. Moritani, T. Hashimoto, and H. Kawai, *Macromolecules*, **4**, 500 (1971).
15. T. Hashimoto, M. Fujimura, K. Saijo, H. Kawai, J. Diamant, and M. Shen, *Advances in Chemistry Series 176*, Am. Chem. Soc., Washington, DC, 1979, p. 257.
16. J. C. Kelterborn and D. S. Soong, *Polym. Eng. Sci.*, **22**, 654 (1982).
17. D. Braun and J. H. Wendorff, *J. Appl. Polym. Sci., Appl. Polym. Symp.*, **39**, 113 (1984).
18. K. Fukumori and T. Kurauchi, *J. Mater. Sci.*, **20**, 1725 (1985).
19. K. Fukumori and T. Kurauchi, *J. Mater. Sci.*, **19**, 2501 (1984).
20. I. M. Ward, *J. Polym. Sci. Symp.*, **58**, 1 (1977).
21. W. Gronski, D. Emeis, A. Brüderlin, M. M. Jacobi, and R. Stadler, *Br. Polym. J.*, **17**, 103 (1985).
22. V. J. McBrierty and D. C. Douglass, *Phys. Rep.*, **63**, 61 (1980).
23. V. J. McBrierty and D. C. Douglass, *J. Polym. Sci. Macromol. Rev.*, **16**, 295 (1981).
24. V. J. McBrierty, *Faraday Disc. Chem. Soc.*, **68**, 78 (1979).
25. D. C. Douglass, *Am. Chem. Soc. Symp. Ser.*, **142**, 147 (1980).
26. H. Tanaka and T. Nishi, *Phys. Rev. B*, **33**, 32 (1986).
27. G. E. Wardell, V. J. McBrierty, and D. C. Douglass, *J. Appl. Phys.*, **45**, 3441 (1974).
28. G. E. Wardell, D. C. Douglass, and V. J. McBrierty, *Polymer*, **17**, 41 (1976).
29. A. C. Lind, *J. Chem. Phys.*, **66**, 3482 (1977).
30. H. Tanaka and T. Nishi, *J. Chem. Phys.*, **82**, 4326 (1985).
31. J. G. Powles and J. H. Strange, *Proc. Phys. Soc. London*, **82**, 6 (1963).
32. H. Y. Carr and E. M. Purcell, *Phys. Rev.*, **94**, 630 (1954).
33. S. Meiboom and D. Gill, *Rev. Sci. Instrum.*, **29**, 688 (1958).
34. H. Takahashi, T. Matsuoka, T. Ohta, K. Fukumori, T. Kurauchi, and O. Kamigaito, *J. Appl. Polym. Sci.*, **36**, 1821 (1988).
35. J. S. Waugh and C. H. Wang, *Phys. Rev.*, **162**, 209 (1967).
36. W. Weibull, *J. Appl. Mech.*, **18**, 293 (1951).
37. S. Kawabata, *Am. Chem. Soc. Symp. Ser.*, **95**, 261 (1979).
38. N. Bloembergen, E. M. Purcell, and R. V. Pound, *Phys. Rev.*, **73**, 679 (1948).
39. R. Kubo and K. Tomita, *J. Phys. Soc. Jpn.*, **9**, 888 (1954).
40. J. H. Van Veck, *Phys. Rev.*, **74**, 1168 (1948).
41. S. Kaufman, W. P. Slichter, and D. D. Davis, *J. Polym. Sci., A-2*, **9**, 829 (1971).
42. H. Tanaka and T. Nishi, *J. Chem. Phys.*, **85**, 6197 (1986).
43. R. Chujo, *Nippon Gomu Kyokaishi*, **31**, 430 (1954).
44. T. Nishi and T. Chikaraishi, *J. Macromol. Sci. Phys.*, **B19**, 445 (1981).
45. G. A. Harpell and C. E. Wilkes, in *Block Polymers*, S. L. Aggarwal, Ed., Plenum, New York, 1970, p. 31.
46. K. Fukumori and T. Kurauchi, to appear.
47. D. C. Douglass, V. J. McBrierty, and T. A. Weber, *Macromolecules*, **10**, 178 (1977).

Received July 26, 1988
Accepted August 25, 1988